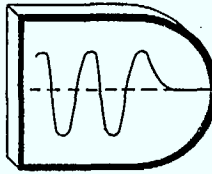


12
AERODYNAMICS
of a
VIBRATING RIBBED STRUCTURE
[DOC-CR-SP-83-024]



PP
9D1
C6555
S55335
19833

checked 11/83



DYNACON Enterprises Ltd.

DYNAMICS AND CONTROL ANALYSIS
18 Cherry Blossom Lane Thornhill, Ontario L3T 3B9 (416) 889-9260

P
91
G655
E5533
1983

②
AERODYNAMICS
of a
VIBRATING RIBBED STRUCTURE
[DOC-CR-SP-83-024]

Industry Canada
LIBRARY
JUL 20 1998
BIBLIOTHÈQUE
Industrie Canada

①
G. B. Sincarsin /
P. C. Hughes

~~COMMUNICATIONS CANADA
MAY 9 1984
LIBRARY - BIBLIOTHÈQUE~~

February 1983

Dynacon Report DAISY-3

P
91
C655
55533
1983

DD 4490191
PL 4490230



Department of Communications

DOC CONTRACTOR REPORT

DOC-CR-SP-83-024

DEPARTMENT OF COMMUNICATIONS - OTTAWA - CANADA

SPACE PROGRAM

TITLE: AERODYNAMICS OF A VIBRATING RIBBED STRUCTURE

AUTHOR(S): G. B. Sincarsin & P. C. Hughes

ISSUED BY CONTRACTOR AS REPORT NO: Dynacon Report DAISY-3

PREPARED BY: Dynacon Enterprises Ltd.
18 Cherry Blossom Lane,
Thornhill, Ontario
L3T 3B9

DEPARTMENT OF SUPPLY AND SERVICES CONTRACT NO: 15ST.36001-2-0727(22ST)

DOC SCIENTIFIC AUTHORITY: A. H. Reynaud (Communications Research Centre)

CLASSIFICATION: Unclassified

This report presents the views of the author(s). Publication of this report does not constitute DOC approval of the reports findings or conclusions. This report is available outside the department by special arrangement.

DATE: February 1983

SUMMARY

Two models for the aerodynamic disturbances experienced by a flexible body moving in a fluid (initially at rest) are presented. The first applies to flows with moderate to high Reynolds numbers and considers the inertial resistance of the fluid. The second deals with viscous effects and low Reynolds number flows. It is demonstrated that the 'inertias' and 'momenta' associated with these models obey parallel-axis theorems analogous to the corresponding structural inertias and momenta for the flexible body. The suitability of both models for use in prediction of the aerodynamic disturbances caused by the laboratory air surrounding DAISY also is assessed.

PREFACE

Acknowledgments

The authors gratefully acknowledge the encouragement and helpful advice of A. H. Reynaud of the Communications Research Centre, who acted as the Scientific Authority for this contract. Thanks are also due Mrs. J. Hughes for typing this report.

Proprietary Rights

Dynacon Enterprises Ltd. does not claim "proprietary rights" to the material in this report. Indeed, the hope is that the analyses, results, ideas and opinions in this report will be useful to others. In this event, a reference to this report would be appreciated.

Units and Spelling

This report uses S.I. units and North American spelling.

TABLE OF CONTENTS

	PAGE
1. INTRODUCTION	1
1.1 Velocity of a Flexible Body Moving Through a Fluid	2
2. INERTIAL RESISTANCE	6
2.1 Neumann's Problem	6
2.2 Form of the Fluid Velocity Potential	7
2.3 Kinetic Energy of the Fluid	8
2.4 Inertial-Resistance Forces and Torques	11
3. VISCOUS RESISTANCE	13
3.1 Creeping Motion Equations	14
3.2 Form of the Fluid Velocity and Pressure	16
3.3 Form of the Pressure Tensor	17
3.4 Hydrodynamic Inertia-Rate and Momentum-Rate Matrices	19
3.5 Viscous-Resistance Forces and Torques	21
4. CONCLUDING REMARKS	22
5. REFERENCES	23
Appendix A - Typical Reynolds Numbers for DAISY	24
Appendix B - Parallel-Axis Theorems for the Hydrodynamic Inertia and Momentum Matrices	30
Appendix C - Parallel-Axis Theorems for the Hydrodynamic Inertia-Rate and Momentum-Rate Matrices	36

LIST OF FIGURES

		PAGE
Figure 1.1:	Comparison of Inertial and Viscous Forces	3
Figure 1.2:	A Flexible Body Immersed in Fluid	4
Figure 3.1a:	Drag Coefficient for Two-Dimensional Bodies	15
Figure 3.1b:	Drag Coefficient for Three-Dimensional Bodies	15
Figure A.1:	Typical Motions for a Rib of DAISY	25
Figure A.2:	Typical Reynolds Numbers for the Rib Vibrations of DAISY	27
Figure A.3:	Flow Regimes as a Function of Frequency and Amplitude	29
Figure B.1:	Geometry of Parallel-Axis Theorems for Hydrodynamic Inertia and Momentum Matrices	31

1. INTRODUCTION

It is well known that environmental disturbances play a key role in the dynamics of spacecraft and that often, in order to achieve some specified level of performance, control strategies must be devised to counteract their effects. To accomplish this end, some reasonable estimate for the various environmental disturbances must be made, based either on analytical models or on flight experience. While for many types of spacecraft this task has been essentially completed, with only the details varying from one design to another, similar progress has yet to be made for structures tested in terrestrial laboratories. In particular, the impact of aerodynamic disturbances on the dynamics of a slowly vibrating body (fundamental frequency < 0.5 Hz.), where the relative velocity between the body and the air is caused solely by the vibratory motion, has not previously been modeled.

While unsteady-flow models do exist for rigid bodies, similar models for flexible bodies are absent in the literature. Unfortunately, it is precisely such models that are required to model the effects of aerodynamic disturbances on DAISY, a highly flexible structure emulating third generation spacecraft (see [Sincarsin (1), 1983]). More than one model is necessary because, for different flow regimes, the importance of inertial and viscous fluid effects will vary.

As with all other fluid dynamics problems, for an immersed flexible body moving unsteadily through a fluid (here, air), the relative importance of viscous drag versus the inertial resistance of the fluid displaced can be assessed by considering the characteristic Reynolds numbers, R , for the motion (translational, R_t , and rotational, R_r),

$$R_t \triangleq \frac{\rho u l_t}{\mu} \quad (1.1)$$

$$R_r \triangleq \frac{\rho \omega l_r^2}{\mu} \quad (1.2)$$

where ρ is the fluid density, μ is the fluid viscosity, u is the translational

velocity (relative to the fluid), ω is the angular velocity (again, relative to the fluid) and ℓ_t and ℓ_r are characteristic lengths associated with the translational and rotational motions. [It is noteworthy that lift can also be generated via viscous effects or by circulation in a potential flow (where inertial effects dominate). These forces are included in what follows.]

Typical Reynolds numbers R for the anticipated rib motions of DAISY are given in Appendix A. They reveal that for certain motions (twist about the rib centerline) viscous effects will dominate, while for other motions (out-of-plane and in-plane displacements) inertial effects may become significant. This does not, however, imply that for twisting motions inertial effects must be ignored, nor that viscous effects are negligible for out-of-plane and in-plane motions. The appropriate aerodynamic disturbance models must be chosen within the context of the original structural model. That is, the situation *could* be as shown in Fig. 1.1, where the inertial fluid forces dominate those caused by viscosity — relative to the corresponding structural forces though, the viscous fluid forces are more important. How well Fig. 1.1 represents reality for DAISY is still to be established. This is part of the ongoing detailed-design procedure documented in [Sincarsin (2), 1983].

To permit a valid assessment of the importance of both inertial and viscous fluid forces, two aerodynamic disturbance models are developed in what follows. The first treats the problem of the inertial resistance generated by a fluid against the unsteady motion of a flexible body immersed in an incompressible frictionless fluid (a model valid for moderate to high R). The second deals with the same motion but does not neglect viscosity and is valid for low R .

1.1 Velocity of a Flexible Body Moving Through a Fluid

Consider a flexible body B immersed in fluid as shown in Fig. 1.2. The body undergoes unsteady motion through a fluid that is initially at rest. The resultant fluid velocity is denoted by $\underline{v}(\underline{r}, t)$, where \underline{r} lies in the region between S_B , the surface of B , and S_∞ , some surface at infinity. The velocity at each point within B is most easily obtained by first considering the displacement at each point and then differentiating with respect to time. Letting

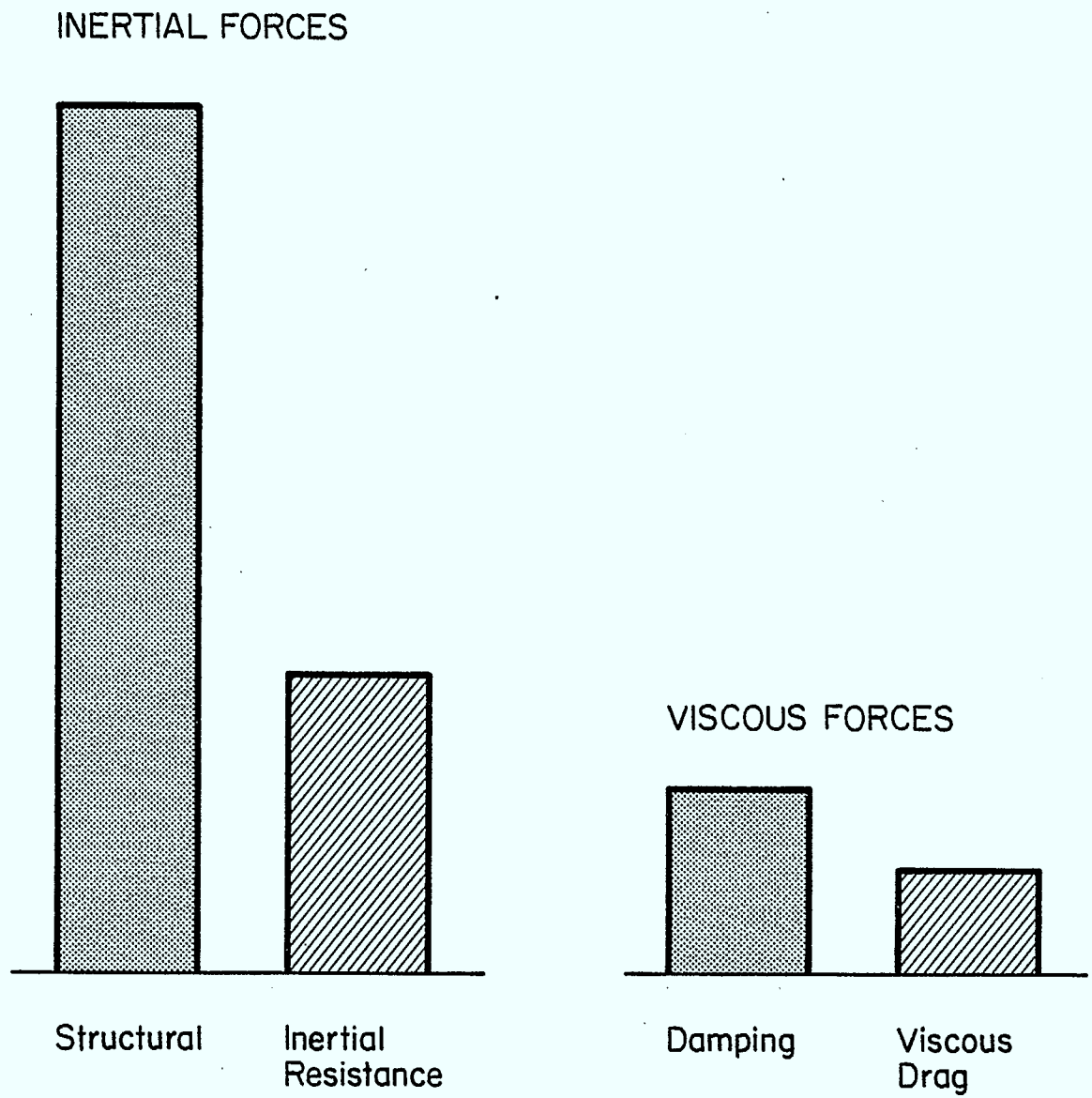


Figure 1.1: Comparison of Inertial and Viscous Forces

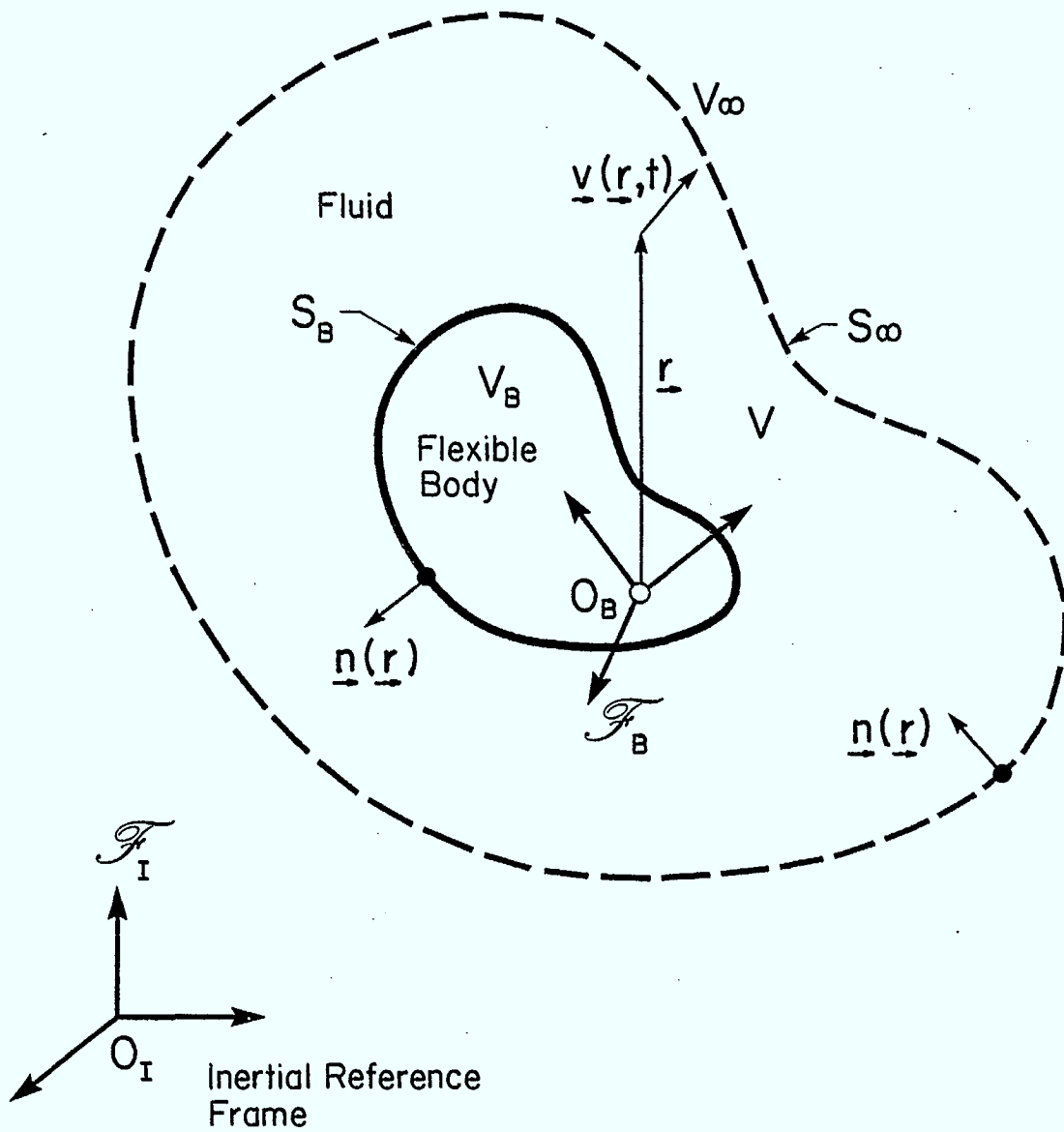


Figure 1.2: A Flexible Body Immersed in Fluid

\underline{w} and $\underline{\theta}$ represent the absolute translational and rotational displacements (first-order infinitesimals) of the reference point O_B (i.e. relative to some inertial frame) and $\underline{\Delta}$ represent the small elastic displacement in body B , the total displacement (to first order) is

$$\underline{d}(\underline{r}, t) = \underline{w}(t) - \underline{r}^X \underline{\theta}(t) + \underline{\Delta}(\underline{r}, t) \quad (1.3)$$

where \underline{r} remains within S_B and \underline{d} is expressed in F_B (see Fig. 1.2). A more useful form of (1.3) is obtained by assuming that $\underline{\Delta}(\underline{r}, t)$ can be expressed as a superposition of 'shape functions' $\underline{\psi}_i(\underline{r})$, each associated with a single 'modal coordinate' $q_i(t)$:

$$\underline{\Delta}(\underline{r}, t) = \sum_{i=1}^{\infty} \underline{\psi}_i(\underline{r}) q_i(t) \quad (1.4)$$

Then, defining a single rectangular matrix $\underline{\Psi}(\underline{r})$ and a single column matrix \underline{q} , as follows,

$$\underline{\Psi}(\underline{r}) \triangleq [\psi_1 \quad \psi_2 \quad \dots] \quad (1.5)$$

$$\underline{q}(t) \triangleq [q_1 \quad q_2 \quad \dots]^T \quad (1.6)$$

(1.3) becomes

$$\underline{d}(\underline{r}, t) = \underline{w}(t) - \underline{r}^X \underline{\theta}(t) + \underline{\Psi}(\underline{r}) \underline{q}(t) \quad (1.7)$$

Whence the velocity at any point in B is

$$\underline{u}(\underline{r}, t) = \dot{\underline{w}}(t) - \underline{r}^X \dot{\underline{\theta}}(t) + \underline{\Psi}(\underline{r}) \dot{\underline{q}}(t) \quad (1.8)$$

expressed in F_B . It is also assumed that the components of $\underline{y}(\underline{r}, t)$ are expressed in F_B in what follows. Furthermore, although B experiences small deformations, it is assumed that its surface area and volume remain constant. The appropriate unit normal vector on $S (=S_B + S_{\infty})$, $\underline{n}(\underline{r}) \mid \underline{r} \in S$, is also shown in Fig. 1.2.

2. INERTIAL RESISTANCE

2.1 Neumann's Problem

Here it is assumed that the fluid, in which the flexible body B shown in Fig. 1.2 is immersed, is incompressible and frictionless (zero viscosity). Furthermore, any fluid motion is induced solely by the motion of B . Now, from the continuity equation for an incompressible fluid (i.e. mass conservation)

$$\underline{\nabla}^T \underline{v} = 0 \quad (2.1)$$

This means we can represent

$$\underline{v} = -\underline{\nabla}\phi \quad (2.2)$$

provided

$$\underline{\nabla}^X \underline{v} = \underline{0} \quad (2.3)$$

that is, provided the flow is irrotational. Furthermore, the fluid velocity potential ϕ is one-valued (only one value of ϕ exists for each \underline{r} in $V (= V_\infty - V_B)$), the volume enclosed by S). From (2.1) and (2.2),

$$\underline{\nabla}^2 \phi = 0 \quad (\underline{\nabla}^2 \equiv \underline{\nabla}^T \underline{\nabla}) \quad (2.4)$$

which is Laplace's equation. Also, the following boundary conditions apply:

$$\underline{v} = \underline{0} \quad \underline{r} \in S_\infty \quad (2.5)$$

$$\underline{n}^T (\underline{u} - \underline{v}) = 0 \quad \underline{r} \in S_B \quad (2.6)$$

Equation (2.6) implies that the flow is ideal. There is tangential 'slip' on the boundary S_B ; however, the velocity components of the body and the fluid normal to S_B must be equal. Now, given (2.2), and (1.8) from the previous section, the boundary conditions (2.5) and (2.6) may be rewritten as

$$\underline{\nabla} \phi = \underline{0} \quad \underline{r} \in S_\infty \quad (2.7)$$

$$\underline{n}^T(\underline{\dot{w}} - \underline{r}^X \underline{\dot{\theta}} + \underline{\psi} \underline{\dot{q}}) = - (\underline{\nabla} \phi)^T \underline{n} = - \frac{\partial \phi}{\partial n} \quad \underline{r} \in S_B \quad (2.8)$$

The problem of solving $\nabla^2 \phi = 0$ within a region, given $\partial \phi / \partial n$ on the boundary, is known as *Neumann's Problem*. Some properties of this problem are as follows:

1. It has a unique solution, hence a unique flow field exists.
2. The maximum or minimum of ϕ must occur on a boundary (S_B or S_∞).
3. Adding a constant to ϕ is irrelevant.
4. The mean value of ϕ over any spherical surface of radius ϵ , is equal to the value of ϕ at the center of the sphere, as $\epsilon \rightarrow 0$.
5. The magnitude of \underline{v} ($= v$) cannot have a maximum at an interior point of the flow field.

2.2 Form of the Fluid Velocity Potential

We note that Laplace's equation (2.4) is a *linear* differential equation, and thus the solution $\phi(\underline{r}, t)$ can be written as a superposition of other solutions. Accordingly, we choose

$$\phi(\underline{r}, t) = \underline{\xi}_W^T(\underline{r}) \underline{\dot{w}}(t) + \underline{\xi}_\theta^T(\underline{r}) \underline{\dot{\theta}}(t) + \underline{\xi}_q^T(\underline{r}) \underline{\psi}(\underline{r}) \underline{\dot{q}}(t) \quad (2.9)$$

with $\underline{\xi}_W$, $\underline{\xi}_\theta$ and $\underline{\xi}_q$ expressed in F_B . Thus, for example, $\underline{\xi}_W$ is the portion of ϕ associated with translational motion. Since, from (2.8),

$$- \frac{\partial \phi}{\partial n} = \underline{n}^T \underline{\dot{w}} - \underline{n}^T \underline{r}^X \underline{\dot{\theta}} + \underline{n}^T \underline{\psi} \underline{\dot{q}} \quad (2.10)$$

and, from (2.9),

$$- \frac{\partial \phi}{\partial n} = - \frac{\partial \underline{\xi}_W^T}{\partial n} \underline{\dot{w}} - \frac{\partial \underline{\xi}_\theta^T}{\partial n} \underline{\dot{\theta}} - \frac{\partial (\underline{\xi}_q^T \underline{\psi})^T}{\partial n} \underline{\dot{q}} \quad (2.11)$$

we conclude that (on S_B)

$$\frac{\partial \underline{\xi}_W}{\partial n} = -\underline{n} \quad ; \quad \frac{\partial \underline{\xi}_\theta}{\partial n} = -\underline{r}^X \underline{n} \quad ; \quad \frac{\partial}{\partial n} (\underline{\xi}_q^T \underline{\Psi}) = -\underline{\Psi}^T \underline{n} \quad (2.12)$$

Furthermore, since $\nabla^2 \phi = 0$, we have

$$\nabla^2 \underline{\xi}_W = \underline{0} \quad ; \quad \nabla^2 \underline{\xi}_\theta = \underline{0} \quad ; \quad \nabla^2 (\underline{\Psi}^T \underline{\xi}_q) = \underline{0} \quad (2.13)$$

It is noteworthy that $\underline{\xi}_W$, $\underline{\xi}_\theta$ and $\underline{\xi}_q$ depend solely on the body shape and not on its motion. Therefore, given the shape of an undeformed flexible body and a knowledge of the possible deformed modes (via the shape functions), one can solve for $\underline{\xi}_W$, $\underline{\xi}_\theta$ and $\underline{\xi}_q$ once and for all. Then specific motions can be determined by using the superposition cited in (2.9). Surface irregularities are not ignored in the above derivation; they would be reflected in the solutions for $\underline{\xi}_W$, $\underline{\xi}_\theta$ and $\underline{\xi}_q$.

2.3 Kinetic Energy of the Fluid

Preparatory to finding the energy of the fluid, we recall Gauss' divergence theorem

$$\int_S \underline{n}^T \underline{a} \, dS = - \int_V \underline{\nabla}^T \underline{a} \, dV \quad (2.14)$$

(The minus sign arises because of the direction of the normal.) We take, in particular,

$$\underline{a} = \phi \underline{\nabla} \phi \quad (2.15)$$

and recall the identity

$$\underline{\nabla}^T (\phi \underline{\nabla} \phi) = (\underline{\nabla} \phi)^T \underline{\nabla} \phi + \phi \nabla^2 \phi \quad (2.16)$$

Thus, given (2.2) and (2.4),

$$\underline{\nabla}^T (\phi \underline{\nabla} \phi) = v^2 \quad (2.17)$$

Now, using (2.14) with \underline{a} defined by (2.15)

$$\int_S \phi \frac{\partial \phi}{\partial n} \, dS = - \int_V v^2 \, dV \quad (2.18)$$

But the kinetic energy of the fluid is given by

$$T_f \triangleq \frac{1}{2} \rho \int_V v^2 dV \quad (2.19)$$

where ρ is the fluid density, so that we obtain

$$T_f = -\frac{1}{2} \rho \int_S \phi \frac{\partial \phi}{\partial n} dS \quad (2.20)$$

Furthermore, for an infinite fluid bounded internally by the surface of an immersed body (as is the case here), it can be shown [Milne and Thomson, 1955] that the integral in (2.20) vanishes on S_∞ and therefore

$$T_f = -\frac{1}{2} \rho \int_{S_B} \phi \frac{\partial \phi}{\partial n} dS_B \quad (2.21)$$

Given the assumed form for the velocity potential from (2.9), the kinetic energy becomes

$$\begin{aligned} T_f = & \frac{1}{2} \dot{W}^T \underline{M}_R \dot{W} + \frac{1}{2} \dot{W}^T \underline{O}_R \dot{\theta} + \frac{1}{2} \dot{W}^T \underline{P}_R \dot{q} \\ & + \frac{1}{2} \dot{\theta}^T \underline{C}_R \dot{W} + \frac{1}{2} \dot{\theta}^T \underline{J}_R \dot{\theta} + \frac{1}{2} \dot{\theta}^T \underline{H}_R \dot{q} \\ & + \frac{1}{2} \dot{q}^T \underline{Q}_R \dot{W} + \frac{1}{2} \dot{q}^T \underline{R}_R \dot{\theta} + \frac{1}{2} \dot{q}^T \underline{M}_{RR} \dot{q} \end{aligned} \quad (2.22)$$

where

$$\begin{aligned} \underline{M}_R & \triangleq -\rho \int_{S_B} \underline{\xi}_W \frac{\partial \underline{\xi}_W^T}{\partial n} dS_B & ; & & \underline{C}_R & \triangleq -\rho \int_{S_B} \underline{\xi}_\theta \frac{\partial \underline{\xi}_W^T}{\partial n} dS_B \\ \underline{O}_R & \triangleq -\rho \int_{S_B} \underline{\xi}_W \frac{\partial \underline{\xi}_\theta^T}{\partial n} dS_B & ; & & \underline{J}_R & \triangleq -\rho \int_{S_B} \underline{\xi}_\theta \frac{\partial \underline{\xi}_\theta^T}{\partial n} dS_B \\ \underline{P}_R & \triangleq -\rho \int_{S_B} \underline{\xi}_W \frac{\partial (\underline{\Psi}^T \underline{\xi}_q)^T}{\partial n} dS_B & ; & & \underline{H}_R & \triangleq -\rho \int_{S_B} \underline{\xi}_\theta \frac{\partial (\underline{\Psi}^T \underline{\xi}_q)^T}{\partial n} dS_B \end{aligned} \quad (2.23)$$

$$\underline{Q}_R \triangleq -\rho \int_{S_B} (\underline{\Psi}^T \underline{\xi}_q) \frac{\partial \underline{\xi}_w^T}{\partial n} dS_B$$

$$\underline{R}_R \triangleq -\rho \int_{S_B} (\underline{\Psi}^T \underline{\xi}_q) \frac{\partial \underline{\xi}_\theta^T}{\partial n} dS_B \quad (2.23)$$

(cont'd)

$$\underline{M}_{RR} \triangleq -\rho \int_{S_B} (\underline{\Psi}^T \underline{\xi}_q) \frac{\partial (\underline{\Psi}^T \underline{\xi}_q)^T}{\partial n} dS_B$$

Now, certain properties of these matrices can be made clear if we again take the divergence theorem (2.14), but instead choose

$$\underline{a} = \phi_1 \underline{\nabla} \phi_2 \quad (2.24)$$

where ϕ_1 and ϕ_2 are any two solutions to Laplace's equation:

$$\nabla^2 \phi_1 = 0 \quad ; \quad \nabla^2 \phi_2 = 0 \quad (2.25)$$

Then

$$\underline{\nabla}^T \underline{a} = (\underline{\nabla} \phi_1)^T \underline{\nabla} \phi_2 - \phi_1 \nabla^2 \phi_2 = (\underline{\nabla} \phi_1)^T \underline{\nabla} \phi_2 \quad (2.26)$$

so that

$$\int_S \phi_1 \frac{\partial \phi_2}{\partial n} dS = - \int_V (\underline{\nabla} \phi_1)^T \underline{\nabla} \phi_2 dV \quad (2.27)$$

However, interchanging ϕ_1 and ϕ_2 gives

$$\int_S \phi_2 \frac{\partial \phi_1}{\partial n} dS = - \int_V (\underline{\nabla} \phi_2)^T \underline{\nabla} \phi_1 dV \quad (2.28)$$

from which the *reciprocity theorem* follows:

$$\int_S \phi_1 \frac{\partial \phi_2}{\partial n} dS = \int_S \phi_2 \frac{\partial \phi_1}{\partial n} dS \quad (2.29)$$

One immediate conclusion from (2.29) is that \underline{M}_R , \underline{J}_R and \underline{M}_{RR} are symmetric matrices. Also, application of (2.29) on a component-by-component basis to the matrix pairs $(\underline{Q}_R, \underline{C}_R)$, $(\underline{Q}_R, \underline{P}_R)$ and $(\underline{R}_R, \underline{H}_R)$ reveals that

$$\begin{aligned}\underline{Q}_R &= \underline{C}_R^T \\ \underline{Q}_R &= \underline{P}_R^T \\ \underline{R}_R &= \underline{H}_R^T\end{aligned}\tag{2.30}$$

Finally, the matrices given in (2.33) can be written in a more compact form by applying (2.12):

$$\begin{aligned}\underline{M}_R &= \rho \int_{S_B} \underline{n} \underline{\xi}_W^T dS_B & ; & & \underline{P}_R &= \rho \int_{S_B} \underline{n} \underline{\xi}_q^T \underline{\psi} dS_B \\ \underline{C}_R &= \rho \int_{S_B} \underline{r}^X \underline{n} \underline{\xi}_W^T dS_B & ; & & \underline{H}_R &= \rho \int_{S_B} \underline{r}^X \underline{n} \underline{\xi}_q^T \underline{\psi} dS_B \\ \underline{J}_R &= \rho \int_{S_B} \underline{r}^X \underline{n} \underline{\xi}_0^T dS_B & ; & & \underline{M}_{RR} &= \rho \int_{S_B} \underline{\psi}^T \underline{n} \underline{\xi}_q^T \underline{\psi} dS_B\end{aligned}\tag{2.31}$$

It is shown in Appendix B that, in fact, *parallel-axis theorems* exist for the fluid inertia and momentum matrices (2.31) that are analogous to their counterparts for the flexible body. The particular forms for the integrals in (2.31) were chosen to permit direct comparison of Appendix B with [Hughes, 1980].

2.4 Inertial-Resistance Forces and Torques

To determine the inertial-resistance forces and torques on body B, all that remains is to apply Lagrange's equation to the system energies:

$$d(\partial L / \partial \dot{\underline{\gamma}}) / dt - \partial L / \partial \underline{\gamma} = \underline{f}_Y\tag{2.32}$$

where

$$L = T - V\tag{2.33}$$

$$T = T_B + T_f \quad (2.34)$$

$$V = V_B \quad (2.35)$$

Here, the total kinetic energy T consists of the kinetic energy of the flexible body, T_B , and the kinetic energy of the fluid, T_f . There is no potential energy associated with the fluid; hence the total potential energy V is simply V_B , the potential energy for body B . The generalized forces associated with each degree of freedom contained in $\underline{\gamma}$ are denoted by \underline{f}_γ . Typically \underline{f}_γ consists of those external forces and torques acting on B that are not implied by V_B ; however, should body B , in fact, be connected to other structural elements (see, for example [Sincarsin (2), 1983]), then \underline{f}_γ will contain interbody forces and torques as well. The exact forms for T_B and V_B are not of interest here — it is only necessary to acknowledge their existence.

Upon substitution of (2.33) through (2.35) into (2.32) and partitioning $\underline{\gamma}$ according to

$$\underline{\gamma} = \text{col}\{\underline{w}, \underline{\theta}, \underline{q}\} \quad (2.36)$$

it follows that

$$d(\partial T_B / \partial \dot{\underline{w}}) / dt - \partial V_B / \partial \underline{w} = \underline{f}_w + \underline{f}_R \quad (2.37)$$

$$d(\partial T_B / \partial \dot{\underline{\theta}}) / dt - \partial V_B / \partial \underline{\theta} = \underline{f}_\theta + \underline{q}_R \quad (2.38)$$

$$d(\partial T_B / \partial \dot{\underline{q}}) / dt - \partial V_B / \partial \underline{q} = \underline{f}_q + \underline{f}_R \quad (2.39)$$

where the inertial-resistance force \underline{f}_R , torque \underline{q}_R , and generalized 'elastic' force \underline{f}_R are

$$\underline{f}_R = -d(\partial T_f / \partial \dot{\underline{w}}) / dt$$

$$\underline{q}_R = -d(\partial T_f / \partial \dot{\underline{\theta}}) / dt \quad (2.40)$$

$$\underline{f}_R = -d(\partial T_f / \partial \dot{\underline{q}}) / dt$$

Then, application of (2.40) to (2.22) of the previous section yields the desired result:

$$\begin{bmatrix} \underline{f}_R \\ \underline{g}_R \\ \underline{f}_R \end{bmatrix} = - \begin{bmatrix} \underline{M}_R & \underline{C}_R^T & \underline{F}_R \\ \underline{C}_R & \underline{J}_R & \underline{H}_R \\ \underline{F}_R^T & \underline{H}_R^T & \underline{M}_{RR} \end{bmatrix} \begin{bmatrix} \ddot{\underline{w}} \\ \ddot{\underline{\theta}} \\ \ddot{\underline{q}} \end{bmatrix} \quad (2.41)$$

The similarity between (2.41) and the corresponding inertial terms associated with the structural mass of body B (see [Sincarsin (2), 1983]) is immediately obvious.

3. VISCOUS RESISTANCE

Generally, the viscous drag on a body is represented via the relation

$$\underline{f}_D = -\frac{1}{2} \rho v^2 C_D \hat{\underline{A}} \underline{\hat{v}} \quad (3.1)$$

where ρ is the fluid density, \underline{v} is the velocity of the fluid flow past the body immersed in the fluid (it has magnitude v and direction $\hat{\underline{v}} = \underline{v}/v$), A is the surface area of the body exposed to the flow (projected perpendicular to $\hat{\underline{v}}$) and C_D is the drag coefficient (a function of Reynolds number, R). For our situation, \underline{v} is not constant in either magnitude or direction over the surface area S_B . Furthermore, since different values of R will apply over different portions of the body (for example, see Appendix A), C_D also varies over S_B . All this suggests that an alternate form for (3.1) should prove more useful:

$$\underline{f}_D = \int_{S_B} d\underline{f}_D \quad (3.2)$$

where

$$d\underline{f}_D = \frac{1}{2} \rho v^2 C_D (\hat{\underline{v}}^T \underline{n}) \hat{\underline{v}} dS_B \quad (3.3)$$

and, as before, \underline{n} is the outward unit normal to the elemental area dS_B . That is,

$$dA = \cos \Lambda dS_B \quad (3.4)$$

where

$$\cos\Lambda = -\hat{\underline{v}}^T \underline{n} \quad (3.5)$$

It is noteworthy, that for C_D and \underline{v} constant, (3.1) is recovered from (3.2) and (3.3).

Since \underline{f}_D does not have to be evaluated relative to the center of pressure—for example, we choose to evaluate \underline{f}_D relative to O_B (recall Fig. 1.2) —a viscous torque also will exist in general:

$$\underline{g}_D = \int_{S_B} \underline{r}^X d\underline{f}_D \quad \underline{r} \in S_B \quad (3.6)$$

Finally, using the concept of virtual work, the generalized 'elastic' drag force acting on a flexible body B is

$$\underline{f}_D = \int_{S_B} \underline{\Psi}(\underline{r})^T d\underline{f}_D \quad \underline{r} \in S_B \quad (3.7)$$

where $\underline{\Psi}(\underline{r})$ is given by (1.5).

While (3.2), (3.6) and (3.7) are valid for all \mathbb{R} , they are somewhat misleading when one attempts to assess the dependence of the drag 'forces' on the velocity \underline{v} . While for low Reynolds numbers C_D is approximately inversely proportional to \underline{v} (see Fig. 3.1) so that the drag 'forces' are essentially *linear* in v , for high Reynolds numbers C_D is almost constant (see Fig. 3.1) and thus the drag 'forces' are virtually *quadratic* in v . Furthermore, for our application it is assumed that \underline{v} is a first-order infinitesimal, since the fluid velocity is induced by motion of the flexible body, which possesses a first-order infinitesimal velocity \underline{u} . As a consequence, for high \mathbb{R} , viscous drag should be a second-order effect. Hence we should concentrate our efforts towards developing a viscous drag model for low- \mathbb{R} flows. Such a model is presented in the following.

3.1 Creeping Motion Equations

For flow with low \mathbb{R} ($\mathbb{R} < 50$) it is reasonable to neglect inertial effects in the general Navier-Stokes fluid equations, in the same way that for

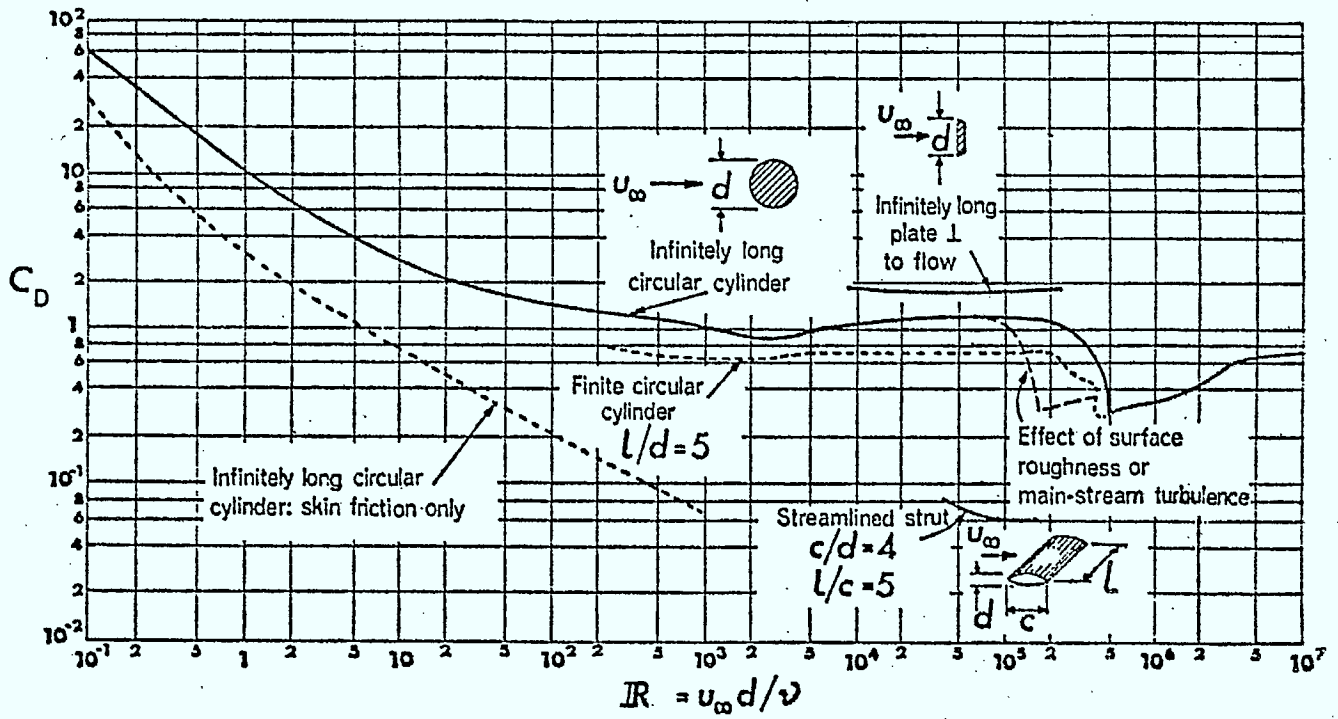


Figure 3.1a: Drag Coefficient for Two-Dimensional Bodies
(from, [Massey, 1970])

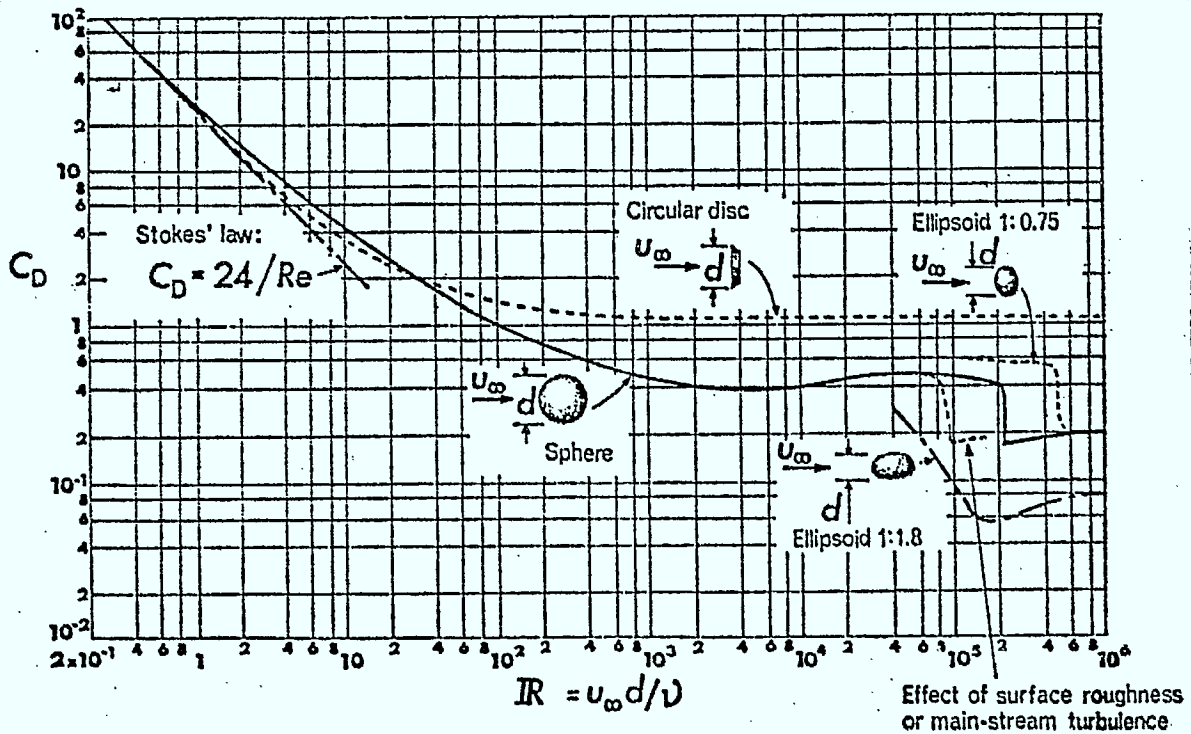


Figure 3.1b: Drag Coefficient for Three-Dimensional Bodies
(from, [Massey, 1970])

high \mathbb{R} ($\mathbb{R} > 10^3$) viscous effects are neglected to obtain potential flow theory (i.e. the theory used in Section 2). If one then assumes the flow to be incompressible, the *creeping motion equations* result:

$$\nabla^2 \underline{v} = \frac{1}{\mu} \nabla p \quad (3.8)$$

$$\nabla^T \underline{v} = 0 \quad (3.9)$$

The pressure on the fluid-body boundary S_B is denoted by p , while the fluid viscosity is represented by μ . Furthermore, for the flexible body B shown in Fig. 1.2, the following boundary conditions apply

$$\underline{v} = \underline{0} \quad \underline{r} \in S_\infty \quad (3.10)$$

$$\underline{v} = \underline{u} \quad \underline{r} \in S_B \quad (3.11)$$

where \underline{u} , the velocity of B , is given by (1.8):

$$\underline{u}(\underline{r}, t) = \dot{\underline{w}}(t) - \underline{r}^X \dot{\underline{\theta}}(t) + \underline{\psi}(\underline{r}) \dot{\underline{q}}(t) \quad (3.12)$$

Equation (3.11) implies that there is no 'slip' on S_B . Unlike the boundary condition for potential flow, both the tangential and the normal velocity components of \underline{v} and \underline{u} must be equal on the surface of the body.

Equations (3.8) through (3.11) are also applicable to unsteady motions [Happel and Brenner, 1973], provided both the translational and rotational \mathbb{R} are small (see Section 1). It is also assumed that the hydrostatic pressure is negligible and that p represents only the dynamic pressure. For our problem, the hydrostatic pressure is essentially constant, since there is no fluid flow without motion of the body.

3.2 Form of the Fluid Velocity and Pressure

The creeping motion equations are *linear* differential equations, and therefore it is possible to seek solutions of the form

$$\underline{v} = \underline{V}_w \dot{\underline{w}} + \underline{V}_\theta \dot{\underline{\theta}} + \underline{V}_q \dot{\underline{q}} \quad (3.13)$$

$$p = \mu (\underline{p}_w \dot{\underline{w}} + \underline{p}_\theta \dot{\underline{\theta}} + \underline{p}_q \dot{\underline{q}}) \quad (3.14)$$

which are superpositions involving the two-dimensional velocity fields \underline{V}_z , $z \in \{w, \theta, q\}$ and the one-dimensional pressure fields \underline{p}_z associated with the translational, rotational and elastic motions of B .

Substitution of (3.13) and (3.14) into (3.8) through (3.11) yields three sets of independent equations, one associated with each type of motion:

$$\begin{aligned} [\nabla^2(\underline{V}_z \underline{A}_z) - \nabla(\underline{p}_z \underline{A}_z)] \dot{\underline{z}} &= \underline{0} \\ [\underline{\nabla}^T(\underline{V}_z \underline{A}_z)] \dot{\underline{z}} &= 0 \\ [(\underline{V}_z - \underline{B}_z) \underline{A}_z] \dot{\underline{z}} &= \underline{0} \quad \underline{r} \in S_B \\ [\underline{V}_z \underline{A}_z] \dot{\underline{z}} &= \underline{0} \quad \underline{r} \in S_\infty \end{aligned} \tag{3.15}$$

where, for $z = (w, \theta, q)$, we set, respectively, $[\underline{A}_z, \underline{B}_z] = ([\underline{1}, \underline{1}], [\underline{1}, -r^X], [\underline{\psi}, \underline{1}])$ and $\underline{1}$ is the identity matrix. However, since (3.15) must be true for all $\dot{\underline{w}}$, $\dot{\underline{\theta}}$ and $\dot{\underline{q}}$, it follows that

$$\begin{aligned} \nabla^2(\underline{V}_z \underline{A}_z) &= \nabla(\underline{p}_z \underline{A}_z) \\ \underline{\nabla}^T(\underline{V}_z \underline{A}_z) &= \underline{0}^T \\ (\underline{V}_z - \underline{B}_z) \underline{A}_z &= \underline{0} \quad \underline{r} \in S_B \\ \underline{V}_z \underline{A}_z &= \underline{0} \quad \underline{r} \in S_\infty \end{aligned} \tag{3.16}$$

Hence, since \underline{V}_z and \underline{p}_z depend solely on the shape of B and not its motion, (3.16) can be solved given the undeformed shape of B and the shape functions associated with its deformed modes. Specific motions can then be represented by applying superposition according to (3.13) and (3.14). Again, surface irregularities will be reflected in the solutions for \underline{V}_z and \underline{p}_z .

3.3 Form of the Pressure Tensor

In an ideal fluid the force exerted on an elemental area dS_B is a

normal thrust proportional to the pressure

$$df_{SB} = -p \underline{n} dS_B \quad (3.17)$$

We can therefore regard the stress (force per unit area) as being obtained from a stress tensor

$$\underline{\Pi} = -p \underline{1} \quad (3.18)$$

whereby

$$df_{SB} = \underline{\Pi}^T \underline{n} dS_B \quad (3.19)$$

For a viscous fluid, the stress tensor is no longer given by (3.18), nor is it in general symmetric, but instead takes the form [Happel and Brenner, 1973]

$$\underline{\Pi} = -p \underline{1} + \kappa (\underline{\nabla}^T \underline{v}) \underline{1} + 2\mu \underline{\Gamma} \quad (3.30)$$

where κ is the bulk (or volume) viscosity, μ is the shear viscosity (here called the fluid viscosity) and $\underline{\Gamma}$, the rate-of-deformation tensor, is given by

$$\underline{\Gamma} = \frac{1}{2} [\underline{\nabla} \underline{v}^T + (\underline{\nabla} \underline{v}^T)^T] - \frac{1}{3} \underline{1} (\underline{\nabla}^T \underline{v}) \quad (3.21)$$

Since, for creeping motion, $\underline{\nabla}^T \underline{v} = 0$, the relevant stress tensor for the present analysis becomes

$$\underline{\Pi} = -p \underline{1} + \mu [\underline{\nabla} \underline{v}^T + (\underline{\nabla} \underline{v}^T)^T] \quad (3.22)$$

(The reader should be cautioned that, because of the order implied by the use of the $\underline{\nabla}$ operator, $(\underline{\nabla} \underline{v}^T)^T \neq \underline{\nabla} \underline{v}^T$.) In fact, substitution of (3.13) and (3.14) into (3.22) yields an alternate form for the stress tensor that will ultimately prove more useful, namely,

$$\underline{\Pi} = \mu (\underline{\Pi}_w + \underline{\Pi}_\theta + \underline{\Pi}_q) \quad (3.23)$$

where

$$\underline{\Pi}_z = -\underline{1} (p_z^T A_z \dot{z}) + \underline{\nabla} (\dot{z}^T A_z^T \underline{v}_z^T) + [\underline{\nabla} (\dot{z}^T A_z^T \underline{v}_z^T)]^T \quad (3.24)$$

and, as before, for $z = (w, \theta, q)$, we use, respectively, $\underline{A}_z = (\underline{1}, \underline{1}, \underline{\psi})$. Finally, we define the three-dimensional matrix \underline{P}_z according to the relation

$$\underline{\Pi}_z = \underline{P}_z \dot{\underline{z}} \quad (3.25)$$

so that the (i,j,k) element of \underline{P}_z is

$$P_{zijk} = -1_{ij} P_{zm} A_{zmk} + \frac{\partial}{\partial x_i} (A_{zkm} V_{z mj}) + \frac{\partial}{\partial x_j} (A_{zkm} V_{z mi}) \quad (3.26)$$

with the repeated index m implying summation over $m = (1,2,3)$, whereupon (3.24) can be written as

$$\underline{\Pi} = \mu (\underline{P}_w \dot{\underline{w}} + \underline{P}_\theta \dot{\underline{\theta}} + \underline{P}_q \dot{\underline{q}}) \quad (3.27)$$

The multiplication operation cited in (3.25) is most easily visualized in indicial notation. Simply,

$$\Pi_{zij} = P_{zijk} \dot{z}_k \quad (3.28)$$

where the range for k is the dimension of \underline{z}_k and the summation convention mentioned previously applies.

3.4 Hydrodynamic Inertia-Rate and Momentum-Rate Matrices

As stated at the beginning of the previous section, the force exerted on an elemental area dS_B is given by

$$d\underline{f}_{SB} = \underline{\Pi}^T \underline{n} dS_B \quad (3.29)$$

where, in our case, $\underline{\Pi}$ is given by (3.27). Hence the total force, torque and generalized 'elastic' force acting on B as it moves in a viscous fluid are

$$\underline{f}_V = \int_{S_B} \underline{\Pi}^T \underline{n} dS_B \quad ; \quad \underline{a}_V = \int_{S_B} \underline{r}^X \underline{\Pi}^T \underline{n} dS_B \quad (3.30)$$

$$\underline{f}_V = \int_{S_B} \underline{\psi}^T \underline{\Pi}^T \underline{n} dS_B$$

These relations can be verified by forming the virtual work expression

$$\delta W = \int_{S_B} \delta \underline{d}(\underline{r}, t)^T d\underline{f}_{SB} \quad (3.31)$$

where the virtual displacement $\delta \underline{d}(\underline{r}, t)$ corresponds to the displacement given by (1.3). Now, recognizing that the i -th element of $\underline{n}_z = \underline{\Pi}_z^T \underline{n}$ is

$$n_{zi} = n_m \Pi_{zmi} \quad (3.32)$$

so that one can define the matrix \underline{N}_z according to

$$N_{zij} \triangleq n_m P_{zmi} \quad (3.33)$$

equations (3.30) can be expanded in terms of the stress tensor (3.27) to obtain

$$\begin{bmatrix} \underline{f}_V \\ \underline{g}_V \\ \underline{h}_V \end{bmatrix} = - \begin{bmatrix} \underline{M}_V & \underline{O}_V & \underline{P}_V \\ \underline{C}_V & \underline{J}_V & \underline{H}_V \\ \underline{Q}_V & \underline{R}_V & \underline{M}_{VV} \end{bmatrix} \begin{bmatrix} \dot{\underline{w}} \\ \dot{\underline{\theta}} \\ \dot{\underline{q}} \end{bmatrix} \quad (3.34)$$

where

$$\begin{aligned} \underline{M}_V &\triangleq - \mu \int_{S_B} \underline{N}_w dS_B & ; & & \underline{C}_V &\triangleq - \mu \int_{S_B} \underline{r}^x \underline{N}_w dS_B \\ \underline{O}_V &\triangleq - \mu \int_{S_B} \underline{N}_\theta dS_B & ; & & \underline{J}_V &\triangleq - \mu \int_{S_B} \underline{r}^x \underline{N}_\theta dS_B \\ \underline{P}_V &\triangleq - \mu \int_{S_B} \underline{N}_q dS_B & ; & & \underline{H}_V &\triangleq - \mu \int_{S_B} \underline{r}^x \underline{N}_q dS_B \\ & & & & \underline{Q}_V &\triangleq - \mu \int_{S_B} \underline{\Psi}^T \underline{N}_w dS_B \end{aligned} \quad (3.35)$$

$$\begin{aligned} \underline{R}_V &\triangleq -\mu \int_{S_B} \underline{\Psi}^T \underline{N}_\theta \, dS_B \\ \underline{M}_{VV} &\triangleq -\mu \int_{S_B} \underline{\Psi}^T \underline{N}_q \, dS_B \end{aligned} \quad \begin{array}{l} (3.35) \\ (\text{cont'd}) \end{array}$$

Various properties of these matrices can be demonstrated by invoking the reciprocal theorem for creeping motion [Happel and Brenner, 1973]:

$$\int_S \underline{v}_2^T \underline{N}_{V_1} \underline{v}_1 \, dS = \int_S \underline{v}_1^T \underline{N}_{V_2} \underline{v}_2 \, dS \quad (3.36)$$

One immediate consequence is that, by choosing the $(\underline{v}, \underline{N}_v)$ pairs in the combinations $(\underline{v}_1, \underline{N}_{V_1}, \underline{v}_2, \underline{N}_{V_2}) = (\dot{\underline{w}}_1, \underline{N}_w, \dot{\underline{w}}_2, \underline{N}_w)$, then $= (-\underline{r}^{X\dot{\theta}}_1, \underline{N}_\theta, -\underline{r}^{X\dot{\theta}}_2, \underline{N}_\theta)$, and finally $= (\underline{\Psi}\dot{\underline{q}}_1, \underline{N}_q, \underline{\Psi}\dot{\underline{q}}_2, \underline{N}_q)$, the matrices \underline{M}_V , \underline{J}_V and \underline{M}_{VV} can be shown to be symmetric. That \underline{N}_w , \underline{N}_θ and \underline{N}_q are independent of the fluid velocity has also been used; they are functions only of the shape of B . Furthermore, choosing $(\underline{v}_1, \underline{N}_{V_1}, \underline{v}_2, \underline{N}_{V_2}) = (\dot{\underline{w}}, \underline{N}_w, -\underline{r}^{X\dot{\theta}}, \underline{N}_\theta)$, then $= (\underline{\Psi}\dot{\underline{q}}, \underline{N}_q, \dot{\underline{w}}, \underline{N}_w)$, and finally $= (\underline{\Psi}\dot{\underline{q}}, \underline{N}_q, -\underline{r}^{X\dot{\theta}}, \underline{N}_\theta)$, it can be shown that

$$\begin{aligned} \underline{O}_V &= \underline{C}_V^T \\ \underline{Q}_V &= \underline{P}_V^T \\ \underline{R}_V &= \underline{H}_V^T \end{aligned} \quad (3.37)$$

Finally, \underline{M}_V , \underline{J}_V , \underline{C}_V and \underline{M}_{VV} , henceforth called the hydrodynamic *inertia-rate* matrices, and \underline{P}_V and \underline{H}_V henceforth called the hydrodynamic *momentum-rate* matrices, obey parallel-axis theorems analogous to those for the inertias and momenta of a flexible body (see Appendix C).

3.5 Viscous-Resistance Forces and Torques

Given (3.34) and (3.37), the general form for the viscous-resistance forces and torques acting upon an immersed flexible body are

$$\begin{bmatrix} \underline{f}_V \\ \underline{g}_V \\ \underline{f}_V \end{bmatrix} = - \begin{bmatrix} \underline{M}_V & \underline{C}_V^T & \underline{P}_V \\ \underline{C}_V & \underline{J}_V & \underline{H}_V \\ \underline{P}_V^T & \underline{H}_V^T & \underline{M}_{VV} \end{bmatrix} \begin{bmatrix} \dot{\underline{w}} \\ \dot{\underline{\theta}} \\ \dot{\underline{q}} \end{bmatrix} \quad (3.38)$$

The term viscous-resistance may be somewhat misleading in that (3.38) includes both lift and drag 'forces'; however, drag is expected to be dominant for DAISY. Also, while (3.38) is valid for a single flexible body, if a number of bodies are interconnected, hydrodynamic interaction forces and torques will result. These are not modeled in (3.38), nor are they modeled in the inertial-resistance 'force' equations (2.41). Their region of importance should, however, be localized near the interconnections. Provided this region is small compared to the body size, their effect on the global hydrodynamic 'forces' [those cited in (2.41) and (3.38)] should be minimal.

4. CONCLUDING REMARKS

An attempt has been made to model the important aerodynamic disturbances affecting the dynamics of a flexible body as it vibrates in air. For motions with *small* \mathcal{R} , the *viscous* effects of the air will dominate. As a consequence, a disturbance model based on the fluid creeping motion equations (Stokes flow) is presented. On the other hand, if the resultant air flow has a *large* \mathcal{R} , it is the *inertial* resistance of the air that becomes important — hence the inclusion of a disturbance model for this effect. It would appear, however, that based on Appendix A, the former disturbance model is of greatest interest with regard to the anticipated rib motions of DAISY.

A very useful trait of both disturbance models is that parallel-axis theorems exist for their individual governing matrices. This enables one to express the forces and torques in each model about any arbitrary reference point, a necessity if these disturbing effects are to be included in a consistent manner in the dynamics model for DAISY.

5. REFERENCES

1. Happel, J.
Brenner, H. *Low Reynolds Number Hydrodynamics*, Noordhoff International Publishing, Netherlands, 1973.
2. Hughes, P. C. "Modal Identities for Elastic Bodies, with Application to Vehicle Dynamics and Control," *Journal of Applied Mechanics*, Vol. 47, No. 1, March, 1980.
3. Massey, B. S. *Mechanics of Fluids* (2nd. ed.), Van Nostrand Reinhold, London, 1970.
4. Milne, L. M.
Thomson, C. B. E. *Theoretical Hydrodynamics* (3rd. ed.) MacMillan, London, 1955.
5. Sincarsin, G. B. "Facility to Study the Control of Flexible Space Structures - Conceptual Design," [DOC-CR-SP-83-022], Dynacon Report DAISY-1, January 1983.
6. Sincarsin, G. B. "Facility to Study the Control of Flexible Space Structures - Detailed Design (Preliminary)," [DOC-CR-SP-83-026], Dynacon Report DAISY-5, March, 1983.

Appendix A

Typical Reynolds Numbers for DAISY

In Section 1, two Reynolds numbers were identified, one associated with translational motion

$$R_t = \frac{\rho u \ell_t}{\mu} \quad (A.1)$$

and a second associated with rotational motion

$$R_t = \frac{\rho \omega \ell_r^2}{\mu} \quad (A.2)$$

Recall that ρ is the fluid density, μ the fluid viscosity, u the translational velocity (relative to the fluid), ω the angular velocity (again, relative to the fluid) and ℓ_t and ℓ_r are characteristic lengths associated with the translational and rotational motions.

The primary sources of flexibility for DAISY (see [Sincarsin (1), 1983]) are the springs at the rib roots where the rib is attached to the structure's central hub. These springs permit the ribs to undergo in-plane, out-of-plane and twisting motions as shown in Fig. A.1. Since the struts which interconnect the ribs are 'follower' structural elements, it is the R associated with these rib vibrations that are of greatest interest here. Furthermore, while the struts are geometrically similar to the ribs, they are dimensionally smaller. Thus the R values cited herein should be upper bounds for the entire structure.

A typical DAISY rib (a cylindrical tube) is 1.35 m in length, with an outside diameter of 0.05 m and a wall thickness of 1.6×10^{-3} m. It is anticipated that the amplitude of the in-plane and out-of-plane rib vibrations will be approximately 0.1 m at the rib tip. The angular amplitude of the twist vibration will be about 0.07 rad (4°). This last estimate is consistent with the angular rotation (α) required at the rib root to produce a 0.1m deflection at the rib tip [i.e. $\alpha \doteq 2 \arctan(0.05/1.35) = 4.2^\circ$]. Now, the velocities for typical translational (in-plane and out-of-plane) and rotational (twist) rib

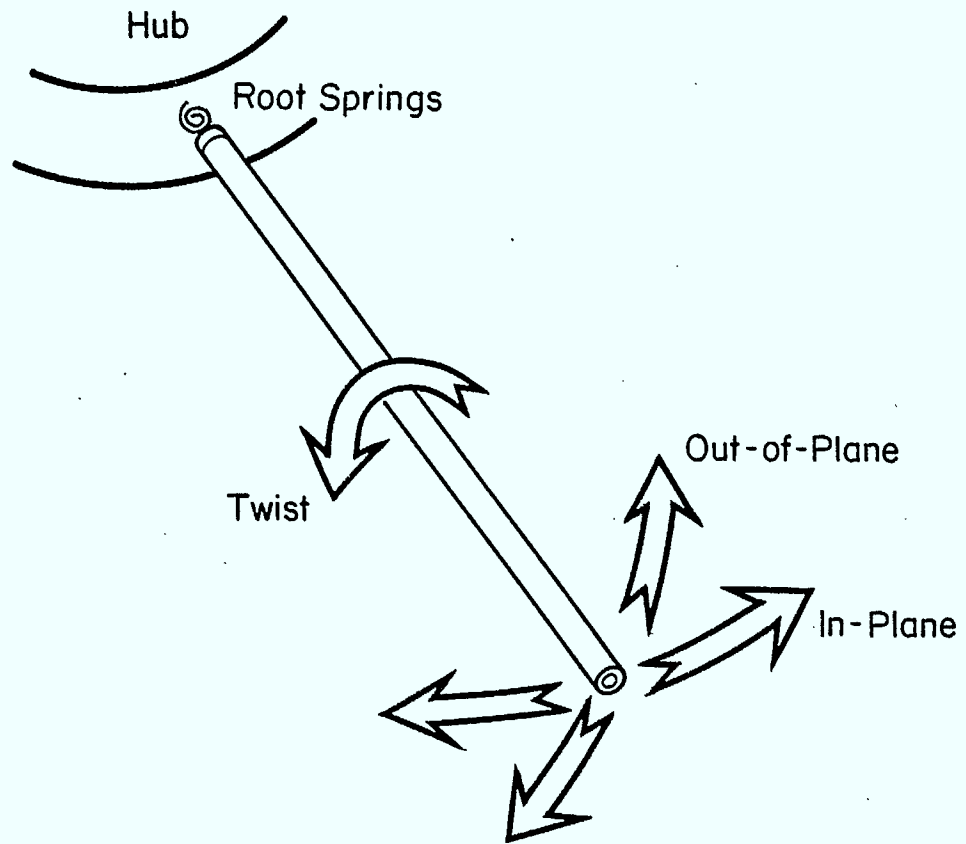


Figure A.1: Typical Motions for a Rib of DAISY

vibrations can be approximated by using the relations

$$u(t) = D_0 \Omega_t \cos \Omega_t t \quad (A.3)$$

$$\omega(t) = \theta_0 \Omega_r \cos \Omega_r t \quad (A.4)$$

where D_0 is the linear amplitude, θ_0 is the angular amplitude and (Ω_t, Ω_r) are the fundamental natural frequencies of the translational and rotational vibrations. The design range for these frequencies is between 0.06 and 3.14 rad/s (see [Sincarsin (1), 1983]). A plot of R_t (evaluated at the rib tip) and R_r versus Ω is provided in Fig. A.2, where (A.1) and (A.2) have been used with

$$u = |u(t)| = D_0 \Omega \quad (A.5)$$

$$\omega = |\omega(t)| = \theta_0 \Omega \quad (A.6)$$

The pertinent values for l_t , l_r , ρ and μ are 0.05 m, 0.05 m, 1.197 kg/m² and 18.22 x 10⁻⁶ kg/ms, where ρ and μ are for dry air at room temperature, 21.5^o C (71^oF). It should be noted that at the rib root, $R_t \equiv 0$.

R_t ranges in value from 20 to 1032, while R_r has the range 0.72 to 36.1. Hence the most important flow regime anticipated for DAISY, from the viewpoint of rib vibrations, has a low R . Viscous effects will dominate for twisting motions. They will also dominate for in-plane and out-of-plane motions if the first natural frequency is near the lower end of the design range. If, however, the first natural frequency occurs near the upper end of the design range then inertia effects may become significant for these two motions. For example, according to Fig. 3.1 of Section 3, $R_t = 1032$ is near the boundary of the R range in which the drag coefficient C_D is approximately constant, that is, the region in which inertial effects dominate.

One shortcoming of Fig. A.2 is that it shows the potential range of R for only the lowest natural frequency. One might inquire as to the consequences of considering a higher value of Ω . In an attempt to answer this question qualitatively, consider (A.1) and (A.2) written explicitly in terms of (A.5) and (A.6), where now Ω is not necessarily the fundamental frequency:

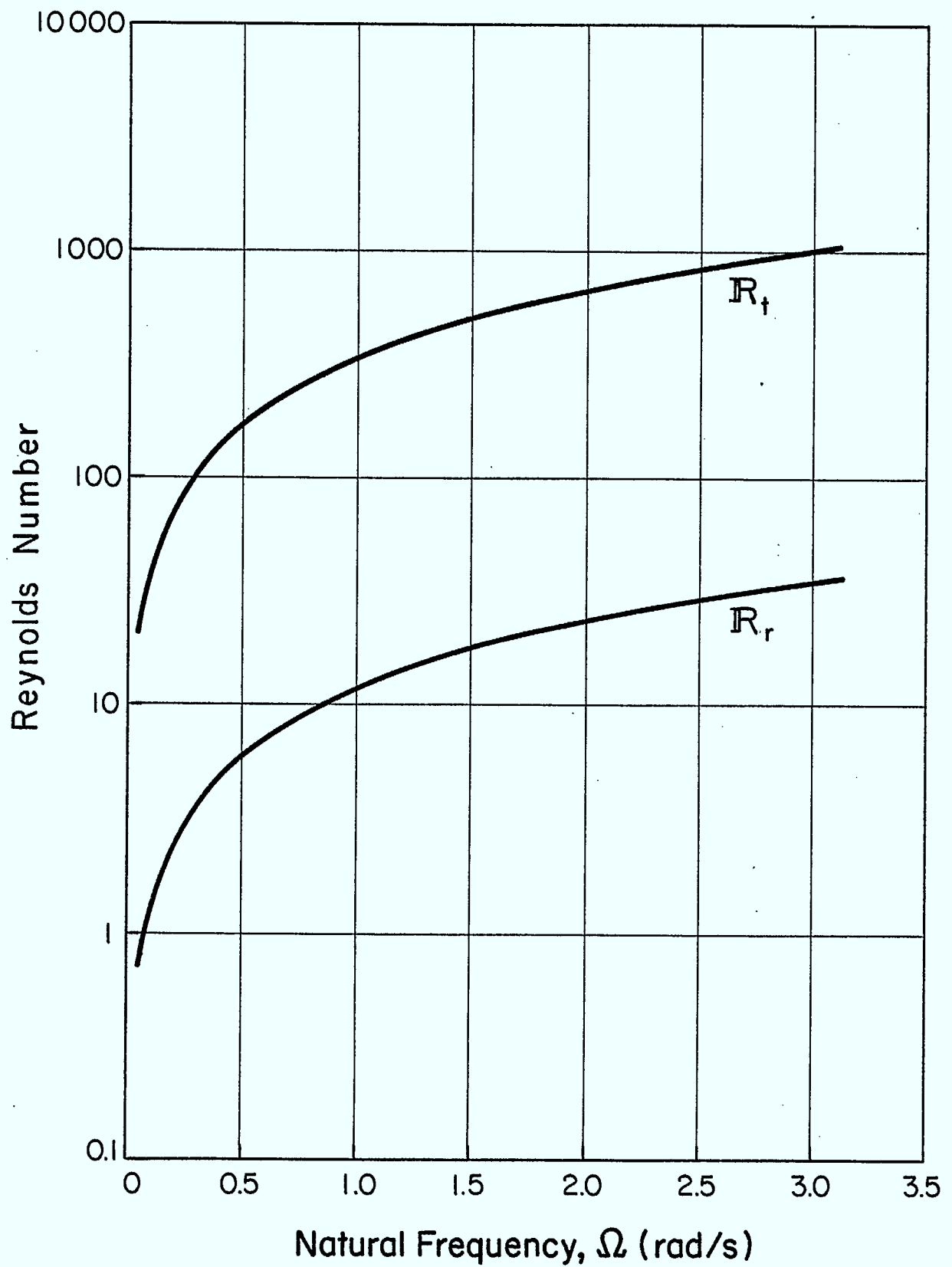


Figure A.2: Typical Reynolds Numbers for the Rib Vibrations of DAISY

$$\mathbb{R}_t = \frac{\rho D_o \Omega_t \ell_t}{\mu} \quad (\text{A.7})$$

$$\mathbb{R}_r = \frac{\rho \theta_o \Omega_r \ell_r^2}{\mu} \quad (\text{A.8})$$

Provided the products $D_o \Omega_t$ and $\theta_o \Omega_r$ remain constant as Ω increases, Fig. A.2 will remain valid. While it is common for the amplitude of vibration for a given body to tend to decrease at the higher natural frequencies, it is not guaranteed that this decrease will exactly equal the increase in frequency. Hence Fig. A.2 may, in fact, underestimate \mathbb{R} for the higher frequencies. It is not expected, however, that this underestimation would be substantial.

One way to confirm that the correct flow regime is being considered is to determine (Ω_t, D_o) and (Ω_r, θ_o) for the frequency range of interest (e.g. the lowest few frequencies of DAISY) and then plot the resulting \mathbb{R} on a frequency-vs-amplitude plot, such as that shown in Fig. A.3. The curves shown in the figure are curves of constant \mathbb{R} ; they are used to demarcate the various flow regimes. Typical values of \mathbb{R} , indicated by crosses, are also shown in the figure. These points could be either analytical predictions or experimental values. As the detailed design progresses, it is hoped that such a plot can be used to confirm that the proper flow regimes have been assumed in formulating aerodynamics disturbance models for DAISY.

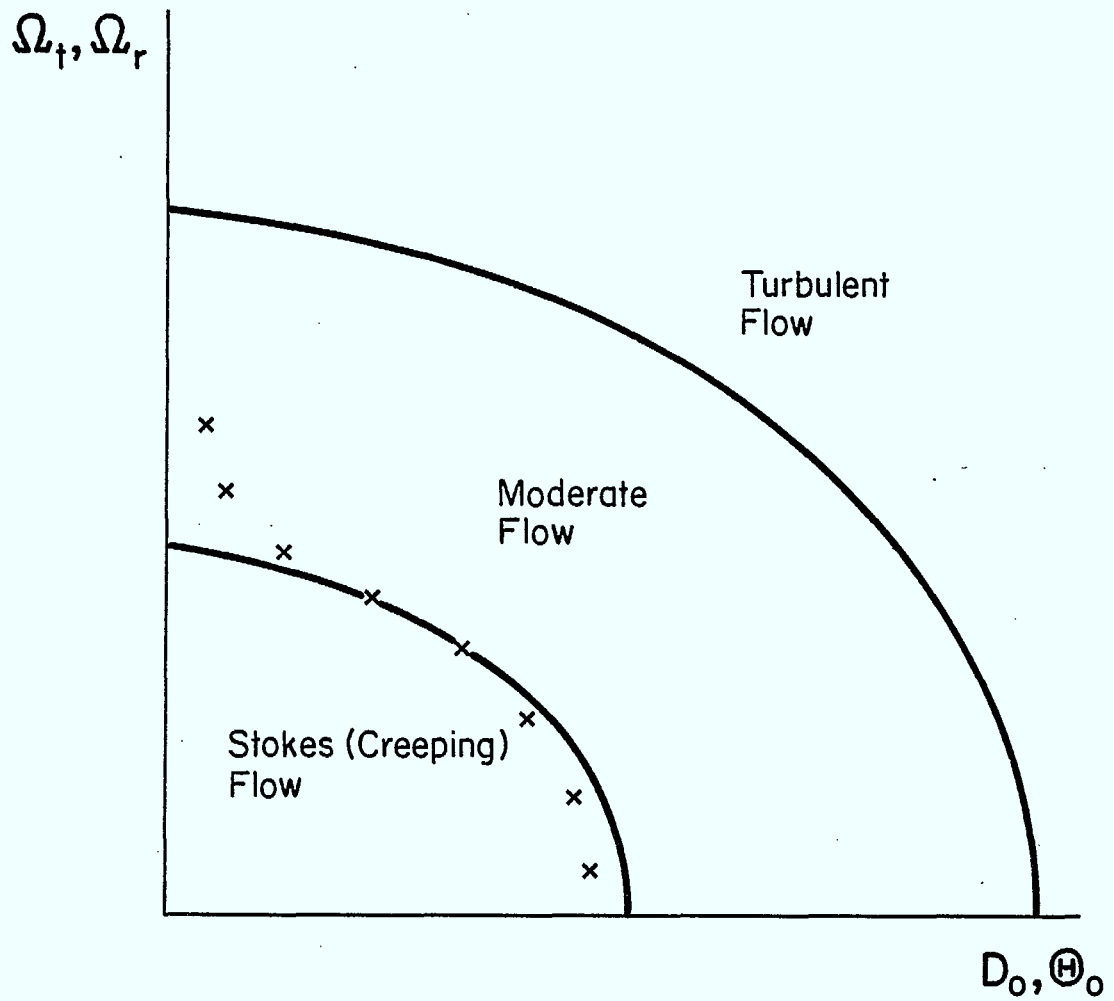


Figure A.3: Flow Regimes as a Function of Frequency and Amplitude

Appendix B

Parallel-Axis Theorems for the Hydrodynamic Inertia and Momentum Matrices

A derivation based on [Hughes, 1980] will be used to prove parallel-axis theorems for the hydrodynamic inertia matrices ($\underline{M}_R, \underline{C}_R, \underline{J}_R, \underline{M}_{RR}$) and momentum matrices ($\underline{P}_R, \underline{H}_R$). These matrices are defined in equation (2.31) of Section 2.

To begin, consider the flexible body shown in Fig. B.1. The two distinct points O_B and O_C are chosen arbitrarily; the only stipulation is that O_C be located relative to O_B by a constant vector \underline{r}_{BC} . The other two vectors, \underline{r}_B and \underline{r}_C , respectively locate an arbitrary point D on the body surface S_B relative to O_B and O_C . Also shown in the figure are the two reference frames F_B and F_C , which have origins at O_B and O_C .

From (1.7) of Section 1.1, we know that the absolute displacement of the point D, in terms of the absolute translational and rotational displacements associated with the frame F_B , is

$$\underline{d}_B(\underline{r}, t) \Big|_{\underline{r} = \underline{r}_B} = \underline{w}_B(t) - \underline{r}_{B-B}^X \theta_B(t) + \underline{\psi}_B(\underline{r}_B) \underline{q}(t) \quad (B.1)$$

where \underline{d}_B is expressed in F_B . Similarly, this same displacement, in terms of the absolute displacements associated with F_C , takes the form

$$\underline{d}_C(\underline{r}, t) \Big|_{\underline{r} = \underline{r}_C} = \underline{w}_C(t) - \underline{r}_{C-C}^X \theta_C(t) + \underline{\psi}_C(\underline{r}_C + \underline{C}_{CB} \underline{r}_{BC}) \underline{q}(t) \quad (B.2)$$

where \underline{d}_C is expressed in F_C and \underline{C}_{CB} is the rotation matrix relating F_B to F_C . Also, since \underline{r}_{BC} is a constant vector, it follows that

$$\underline{w}_C = \underline{C}_{CB} (\underline{w}_B - \underline{r}_{BC}^X \theta_B) \quad (B.3)$$

$$\theta_C = \underline{C}_{CB} \theta_B \quad (B.4)$$

where, as in (B.2) \underline{r}_{BC} is expressed in F_B . Now, forming

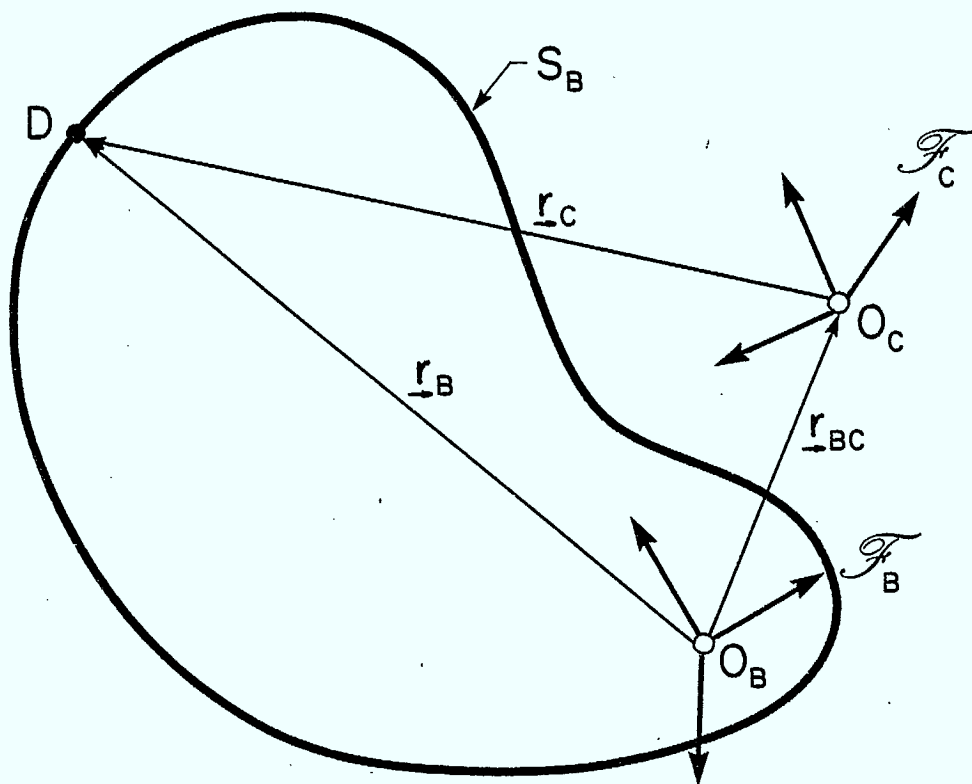


Figure B.1: Geometry of Parallel-Axis Theorems for Hydrodynamic Inertia and Momentum Matrices

$$\underline{d}_C = \underline{C}_{CB} \underline{d}_B \quad (\text{B.5})$$

and applying (B.3) and (B.4), it can be shown that

$$\underline{\Psi}_C(\underline{C}_{CB} \underline{r}_B) = \underline{C}_{CB} \underline{\Psi}_B(\underline{r}_B) \quad (\text{B.6})$$

where the relation

$$\underline{r}_B = \underline{r}_{BC} + \underline{C}_{BC} \underline{r}_C \quad (\text{B.7})$$

(see Fig. B.1) has been used. Here, as in (B.1) and (B.2), \underline{r}_B is expressed in F_B and \underline{r}_C is expressed in F_C . The identity

$$(\underline{C}_{PQ} \underline{r})^X = \underline{C}_{PQ} \underline{r}^X \underline{C}_{QP} \quad (\text{B.8})$$

with

$$\underline{C}_{QP} = \underline{C}_{PQ}^T \quad (\text{B.9})$$

is also required to obtain (B.6). Prior to proceeding, it is useful to note that in what follows the rotation matrix \underline{C}_{BC} can be taken to be constant since it always multiplies a first-order quantity. Hence any first-order change in \underline{C}_{BC} ultimately yields second-order terms, to be neglected in the present analysis.

Let us now consider the velocity potential ϕ at D expressed in terms of the absolute velocities of F_B and F_C

$$\phi_B = \underline{\xi}_{wB} \dot{w}_B + \underline{\xi}_{\theta B}^T \dot{\theta}_B + \underline{\xi}_{qB}^T \underline{\Psi}_B \dot{q}_B \quad (\text{B.10})$$

$$\phi_C = \underline{\xi}_{wC} \dot{w}_C + \underline{\xi}_{\theta C}^T \dot{\theta}_C + \underline{\xi}_{qC}^T \underline{\Psi}_C \dot{q}_C \quad (\text{B.11})$$

In the above, $\underline{\xi}_{zB}$, for $z \in \{w, \theta, q\}$, is expressed in F_B , while $\underline{\xi}_{zC}$ is expressed in F_C . However, ϕ is a scalar and thus independent of reference frame. Therefore, equating (B.10) and (B.11) and applying (B.3), (B.4) and (B.6), one finds that

$$\underline{\xi}_{WB}^T = \underline{\xi}_{WC}^T \underline{C}_{CB} \quad (B.12)$$

$$\underline{\xi}_{OB}^T = \underline{\xi}_{OC}^T \underline{C}_{CB} - \underline{\xi}_{WC}^T \underline{C}_{CB} \underline{r}_{BC}^X \quad (B.13)$$

$$\underline{\xi}_{qB}^T = \underline{\xi}_{qC}^T \underline{C}_{CB} \quad (B.14)$$

These results are essential to the development of the parallel-axis theorems applying to the hydrodynamic inertia and momentum matrices. For example, that \underline{M}_R is independent of the chosen origin can be demonstrated quite readily by application of (B.12). One simply notes, from (2.31) that \underline{M}_R , in terms of quantities related to O_B and expressed in F_B , is

$$\underline{M}_{RB} = \rho \int_{S_B} \underline{n}_B \underline{\xi}_{WB}^T dS_B \quad (B.15)$$

while in terms of quantities related to O_C , \underline{M}_R (expressed in F_C) becomes

$$\underline{M}_{RC} = \rho \int_{S_B} \underline{n}_C \underline{\xi}_{WC}^T dS_B \quad (B.16)$$

where

$$\underline{n}_C = \underline{C}_{CB} \underline{n}_B \quad (B.17)$$

is the outward normal to S_B at the point D expressed in F_C (i.e. \underline{n}_B is the outward normal to S_B at the point D expressed in F_B). By direct substitution of (B.12) into (B.15), and noting (B.17), it follows that

$$\underline{M}_{RB} = \underline{C}_{BC} \underline{M}_{RC} \underline{C}_{CB} \quad (B.18)$$

which confirms the stated independence. The parallel-axis theorem governing the hydrodynamic first-moment-of-inertia matrix can be demonstrated using an analogous procedure. One begins by writing \underline{C}_R (recall (2.31)) in terms of quantities related to O_B and O_C ,

$$\underline{C}_{RB} = \rho \int_{S_B} \underline{r}_{B-B}^X \underline{n}_B \underline{\xi}_{WB}^T dS_B \quad (B.19)$$

$$\underline{C}_{RC} = \rho \int_{S_B} \underline{r}_{C-C}^X n_C \underline{\epsilon}_{WC}^T dS_B \quad (\text{B.20})$$

with \underline{C}_{RB} expressed in F_B and \underline{C}_{RC} expressed in F_C . Then application of (B.12) and (B.7) to (B.19), given (B.8), (B.9), (B.15) and (B.17), produces

$$\underline{C}_{RB} = \underline{C}_{BC} \underline{C}_{RC} \underline{C}_{CB} + \underline{r}_{BC}^X \underline{C}_{BC} \underline{M}_{RC} \underline{C}_{BC} \quad (\text{B.21})$$

Also, it can be shown that for the hydrodynamic second-moment-of-inertia matrix \underline{J}_R ,

$$\begin{aligned} \underline{J}_{RB} &= \underline{C}_{BC} \underline{J}_{RC} \underline{C}_{CB} - \underline{C}_{BC} \underline{C}_{RC} \underline{C}_{CB} \underline{r}_{BC}^X \\ &+ \underline{r}_{BC}^X \underline{C}_{BC} \underline{C}_{RC}^T \underline{C}_{CB} - \underline{r}_{BC}^X \underline{C}_{BC} \underline{M}_{RC} \underline{C}_{CB} \underline{r}_{BC}^X \end{aligned} \quad (\text{B.22})$$

where, from (2.31),

$$\underline{J}_{RB} = \int_{S_B} \underline{r}_{B-B}^X n_B \underline{\epsilon}_{\theta B}^T dS_B \quad (\text{B.23})$$

$$\underline{J}_{RC} = \int_{S_B} \underline{r}_{C-C}^X n_C \underline{\epsilon}_{\theta C}^T dS_B \quad (\text{B.24})$$

To demonstrate (B.22), first (B.13) is substituted into (B.23) and then (B.8), (B.9), (B.15), (B.17) and (B.20) are applied. Finally, (B.6), (B.14) and (B.17) can be used to show that the elastic-mass matrix \underline{M}_{RR} obeys the relation

$$\underline{M}_{RRB} = \underline{M}_{RRC} \quad (\text{B.25})$$

where

$$\underline{M}_{RRB} = \rho \int_{S_B} \underline{\Psi}_B^T n_B \underline{\epsilon}_{qB}^T \underline{\Psi}_B dS_B \quad (\text{B.26})$$

$$\underline{M}_{RRC} = \rho \int_{S_B} \underline{\Psi}_C^T n_C \underline{\epsilon}_{qC}^T \underline{\Psi}_C dS_B \quad (\text{B.27})$$

and, as before, quantities with the subscript B(C) are expressed in $F_{B(C)}$.

For the hydrodynamic momentum matrices

$$\underline{P}_R = \rho \int_{S_B} \frac{n \xi^T \Psi}{q} dS_B \quad (B.28)$$

$$\underline{H}_R = \rho \int_{S_B} \frac{r^X n \xi^T \Psi}{q} dS_B \quad (B.29)$$

the same procedure is followed. First, \underline{P}_R and \underline{H}_R are expressed relative to O_B and O_C and then the appropriate equations from (B.12) through (B.14) are applied to obtain

$$\underline{P}_{RB} = C_{BC} \underline{P}_{RC} \quad (B.30)$$

$$\underline{H}_{RB} = C_{BC} \underline{H}_{RC} + r_{BC}^X C_{BC} \underline{P}_{RC} \quad (B.31)$$

Equation (B.17) is also required for both proofs, while (B.7) is necessary only for \underline{H}_R . It is notable that both (B.30) and (B.31) and the relations governing the hydrodynamic inertia matrices are analogous to those for the corresponding structural momentum and inertia matrices for a general body (see [Hughes, 1980]). In particular, (B.21), (B.22) and (B.31) are the parallel-axis theorems for the hydrodynamic inertia and momentum matrices \underline{C}_R , \underline{J}_R and \underline{H}_R .

Appendix C

Parallel-Axis Theorems for the Hydrodynamic Inertia-Rate and Momentum-Rate Matrices

The geometry governing the equations developed in this appendix is the same as in Appendix B. In this respect, the reader is advised to become acquainted with Fig. B.1 and the notation of Appendix B. Furthermore, the following relations should be noted:

$$\underline{w}_C = \underline{C}_{CB}(\underline{w}_B - \underline{r}_{BC}^x \underline{\theta}_B) \quad (C.1)$$

$$\underline{\theta}_C = \underline{C}_{CB} \underline{\theta}_B \quad (C.2)$$

$$\underline{\psi}_C = \underline{C}_{CB} \underline{\psi}_B \quad (C.3)$$

$$\underline{r}_B = \underline{r}_{BC} + \underline{C}_{BC} \underline{r}_C \quad (C.4)$$

$$\underline{n}_B = \underline{C}_{BC} \underline{n}_C \quad (C.5)$$

Now, from Section 3.4, it can be inferred that the normal component of the stress tensor \underline{n}_π ,

$$\underline{n}_\pi = \underline{\Pi}^T \underline{n} \quad (C.6)$$

can be written as

$$\underline{n}_\pi = \mu (\underline{N}_w \dot{\underline{w}} + \underline{N}_\theta \dot{\underline{\theta}} + \underline{N}_q \dot{\underline{q}}) \quad (C.7)$$

where

$$n_{\pi zi} = n_{m \Pi zmi} = N_{zij} \dot{z}_j \quad (C.8)$$

$$\underline{\Pi}_z = -\underline{1}(\underline{p}_{z-z}^T \underline{\dot{z}}) + \underline{\nabla}(\underline{\dot{z}}^T \underline{A}_{z-z}^T \underline{V}^T) + [\underline{\nabla}(\underline{\dot{z}}^T \underline{A}_{z-z}^T \underline{V}^T)] \quad (C.9)$$

with $\underline{A}_z = (\underline{1}, \underline{1}, \underline{\psi})$, respectively, for $z = (w, \theta, q)$. Hence, the normal component of the stress tensor at the point D (shown in Fig. B.1), in terms of quantities related to O_B , is

$$\underline{n}_{\pi B} = \mu(\underline{N}_{WB}\dot{\underline{w}}_B + \underline{N}_{\theta B}\dot{\underline{\theta}}_B + \underline{N}_{qB}\dot{\underline{q}}) \quad (C.10)$$

where $\underline{n}_{\pi B}$ is expressed in F_B . Similarly, for quantities related to O_C ,

$$\underline{n}_{\pi C} = \mu(\underline{N}_{WC}\dot{\underline{w}}_C + \underline{N}_{\theta C}\dot{\underline{\theta}}_C + \underline{N}_{qC}\dot{\underline{q}}) \quad (C.11)$$

where $\underline{n}_{\pi C}$ is expressed in F_C . However, since (C.10) and (C.11) represent the same vector, it follows that

$$\underline{n}_{\pi C} = \underline{C}_{CB}\underline{n}_{\pi B} \quad (C.12)$$

where \underline{C}_{CB} is the rotation matrix relating F_B to F_C (see Appendix B). Thus, substituting (C.10) and (C.11) into (C.12), and applying (C.1) through (C.3), it can be shown that

$$\underline{N}_{WB} = \underline{C}_{BC}\underline{N}_{WC}\underline{C}_{CB} \quad (C.13)$$

$$\underline{N}_{\theta B} = \underline{C}_{BC}\underline{N}_{\theta C}\underline{C}_{CB} - \underline{C}_{BC}\underline{N}_{WB}\underline{C}_{CB}\underline{r}_{BC}^x \quad (C.14)$$

$$\underline{N}_{qB} = \underline{C}_{BC}\underline{N}_{qC} \quad (C.15)$$

where

$$\underline{C}_{BC} = \underline{C}_{CB}^T \quad (C.16)$$

Relations (C.13) through (C.15) can be confirmed directly using (C.8) and (C.9), as follows. To begin, we express the absolute velocity of the point D in terms of quantities related to O_B and O_C , using (3.13) of Section (3.2):

$$\underline{v}_B = \underline{V}_{WB}\dot{\underline{w}}_B + \underline{V}_{\theta B}\dot{\underline{\theta}}_B + \underline{V}_{qB}\underline{y}_B\dot{\underline{q}} \quad (C.17)$$

$$\underline{v}_C = \underline{V}_{WC}\dot{\underline{w}}_C + \underline{V}_{\theta C}\dot{\underline{\theta}}_C + \underline{V}_{qC}\underline{y}_C\dot{\underline{q}} \quad (C.18)$$

Here the matrices in (C.17) are expressed in F_B , while those in (C.18) are expressed in F_C . The realization that these two equations represent the same vector \underline{v} , combined with (C.1) through (C.3), yields the relations

$$\underline{v}_{wB} = \underline{c}_{BC} \underline{v}_{wC} \underline{c}_{CB} \quad (C.19)$$

$$\underline{v}_{\theta B} = \underline{c}_{BC} \underline{v}_{\theta C} \underline{c}_{CB} - \underline{c}_{BC} \underline{v}_{wC} \underline{c}_{CB} r_{BC}^x \quad (C.20)$$

$$\underline{v}_{qB} = \underline{c}_{BC} \underline{v}_{qC} \underline{c}_{CB} \quad (C.21)$$

Similarly, we can show using (3.14) that the pressure fields \underline{p}_z , $z \in \{w, \theta, q\}$, associated with the pressure at point D satisfy the equations

$$\underline{p}_{wB}^T = \underline{p}_{wC}^T \underline{c}_{CB} \quad (C.22)$$

$$\underline{p}_{\theta B}^T = \underline{p}_{\theta C}^T \underline{c}_{CB} - \underline{p}_{wC}^T \underline{c}_{CB} r_{BC}^x \quad (C.23)$$

$$\underline{p}_{qB}^T = \underline{p}_{qC}^T \underline{c}_{CB} \quad (C.24)$$

Now since, for creeping motion, $\underline{\Pi}$ is symmetric, it follows from (C.8) and (C.9), that

$$\underline{n}_{\pi z} = -\underline{n} \underline{p}_{zA}^T \underline{z} \dot{\underline{z}} + \underline{\nabla} (\underline{z} \underline{A}^T \underline{V}^T) \underline{n} + [\underline{\nabla} (\underline{z} \underline{A}^T \underline{V}^T) \underline{T} \underline{n}] \quad (C.25)$$

If (C.25) is then expressed in quantities related to O_B and O_C and the resulting equations equated using (C.6) (after applying the appropriate rotation matrix) (C.13) through (C.15) can be reproduced, given (C.8). This procedure requires the use of (C.1) through (C.5) as well as (C.19) through (C.21) and (C.22) through (C.24). It is also necessary to employ the gradient identity

$$\underline{v}_B = \underline{c}_{BC} \underline{v}_C \quad (C.26)$$

which follows from the relation

$$\underline{\Pi}_B = \underline{c}_{BC} \underline{\Pi}_C \underline{c}_{CB} \quad (C.27)$$

where $\underline{\Pi}_{B,C}$ is the stress tensor at D written in terms of quantities related to $O_{B,C}$ and expressed in $F_{B,C}$.

Now that the validity of equations (C.13), (C.14) and (C.15) has

been confirmed, they can be used to establish the desired parallel-axis theorems. In this regard, the definitions for the hydrodynamic inertia-rate matrices ($\underline{M}_V, \underline{C}_V, \underline{J}_V$ and \underline{M}_{VV}) and the hydrodynamic momentum-rate matrices (\underline{P}_V and \underline{H}_V) should be recalled from (3.35) of Section 3.4. As in Appendix B, it is straightforward to demonstrate that \underline{M}_V is independent of the chosen origin. Simply write \underline{M}_V in terms of quantities related to O_B (expressed in F_B) and in terms of quantities related to O_C (expressed in F_C),

$$\underline{M}_{VB} = -\mu \int_{S_B} \underline{N}_{WB} dS_B \quad (C.28)$$

$$\underline{M}_{VC} = -\mu \int_{S_B} \underline{N}_{WC} dS_B \quad (C.29)$$

and then apply (C.13) to obtain

$$\underline{M}_{VB} = \underline{C}_{BC} \underline{M}_{VC} \underline{C}_{CB} \quad (C.30)$$

The parallel-axis theorem corresponding to the hydrodynamic first-moment-of-inertia rate matrix \underline{C}_V is likewise demonstrated by applying (C.4) and (C.13) to

$$\underline{C}_{VB} = -\mu \int_{S_B} \underline{r}_{B \rightarrow WB}^X \underline{N}_{WB} dS_B \quad (C.31)$$

$$\underline{C}_{VC} = -\mu \int_{S_B} \underline{r}_{C \rightarrow WB}^X \underline{N}_{WB} dS_B \quad (C.32)$$

where $\underline{C}_{VB,C}$ are defined in a manner analogous to $\underline{M}_{VB,C}$, to obtain

$$\underline{C}_{VB} = \underline{C}_{BC} \underline{C}_{VC} \underline{C}_{CB} + \underline{r}_{BC}^X \underline{C}_{BC} \underline{M}_{VC} \underline{C}_{CB} \quad (C.33)$$

Furthermore, defining

$$\underline{J}_{VB} = -\mu \int_{S_B} \underline{r}_{B \rightarrow \theta B}^X \underline{N}_{WB} dS_B \quad (C.34)$$

$$\underline{J}_{VC} = -\mu \int_{S_B} \underline{r}_{C \rightarrow \theta C}^X N_{\theta C} dS_B \quad (C.35)$$

and noting (C.4), (C.14), (C.28) and (C.32) it can be shown that the hydrodynamic second-moment-of-inertia rate matrix \underline{J}_R obeys the relation

$$\begin{aligned} \underline{J}_{VB} &= \underline{C}_{BC} \underline{J}_{VC} \underline{C}_{CB} - \underline{C}_{BC} \underline{C}_{VC} \underline{C}_{CB} \underline{r}_{BC}^X + \underline{r}_{BC}^X \underline{C}_{BC} \underline{C}_{VC}^T \underline{C}_{CB} \\ &\quad - \underline{r}_{BC}^X \underline{C}_{BC} \underline{M}_{rC} \underline{C}_{BC} \underline{r}_{BC}^X \end{aligned} \quad (C.36)$$

where, as before $\underline{J}_{VB,C}$ refer to \underline{J}_R written in terms of variables related to $O_{B,C}$ and expressed in $F_{B,C}$. Finally, the last inertia-rate matrix, the one associated with the 'elastic mass,' \underline{M}_{VV} , can be shown to satisfy the equation

$$\underline{M}_{VVB} = \underline{M}_{VVC} \quad (C.37)$$

where

$$\underline{M}_{VVB} = -\mu \int_{S_B} \underline{\psi}_B^T N_{qB} dS_B \quad (C.38)$$

$$\underline{M}_{VVC} = -\mu \int_{S_B} \underline{\psi}_C^T N_{qC} dS_B \quad (C.39)$$

by virtue of (C.3) and (C.15).

As in the previous appendix, the relations governing the momentum-rate matrices

$$\underline{P}_V = -\mu \int_{S_B} N_q dS_B \quad (C.40)$$

$$\underline{H}_V = -\mu \int_{S_B} \underline{r}_{rC}^X N_q dS_B \quad (C.41)$$

are obtained by applying the same techniques used for the inertia-rate matrices. Rather than repeat details, only the resulting equations are recorded:

$$\underline{P}_{VB} = \underline{C}_{BC} \underline{P}_{VC} \quad (C.42)$$

$$\underline{H}_{VB} = \underline{C}_{BC} \underline{H}_{VC} + r_{BC}^X \underline{C}_{BC} \underline{P}_{RC} \quad (C.43)$$

Again, the striking similarity between the parallel-axis theorems governing \underline{C}_V , \underline{J}_V and \underline{H}_V and those governing the inertia and momentum matrices for both the fluid (see Appendix B) and the structure (see [Hughes, 1980]) should be noted.



SINCARSIN, G.B.
Aerodynamics of a vibrating
ribbed structure

P
91
C655
S5533
1983

DATE DUE
DATE DE RETOUR

